

Characterization of a Polarisation Based Entangled Photon Source

Y. Ismail^{1,*}, A. R. Mirza^{1,2}, A. Forbes^{1,3} and F. Petruccione^{1,2,4}

¹*University of KwaZulu-Natal, Durban 4000, South Africa*

²*QZN Technology, Innovation Centre, Howard College Campus, University of KwaZulu-Natal, South Africa*

³*CSIR- National Laser Centre, Pretoria 0001, South Africa*

⁴*National Institute for Theoretical Physics, South Africa*

Entanglement is essentially at the core of quantum mechanics and deals with the ability to couple two or more particles in time and space. Entanglement is relevant to all sub-atomic particles which include photons, electrons and ions. The generation of entangled photons is beneficial for the development of quantum communication techniques since it eliminates the possibility of photon number splitting attacks during the key distribution process. This is applicable to both fibre and free-space systems. One of the techniques to obtain an entangled single photon pair lies in the successful implementation of a second-order non-linear process, which is referred to as Spontaneous Parametric Down Conversion (SPDC). Here, we will discuss the procedure that leads to the construction of a polarization-based entangled system and consider some of the measurement techniques, which can be applied to the aforementioned system. This would be realized by characterizing the system and hence verifying quantum correlation by means of, violating the Clauser, Horne, Shimony and Holt (CHSH) inequalities. We discuss in detail the methodology to assembling an entangled source. Furthermore, we quantify the quantum nature of our system by obtaining a violation of 2.71 ± 0.03 . We measure the fidelity of the system to be 0.997 ± 0.0001 , which confirms the quantum states created were preserved.

1. Introduction

Entanglement occurs when two particles interact physically but indistinguishably and thereafter separate, such that knowledge about a distant particle can be obtained by observing its local entangled partner. Einstein, Podolsky and Rosen (EPR) argued that entangled systems contradict the classical notions of both reality and locality [1]. If two physical systems were to interact with respect to a certain observable, then due to this interaction, the two systems would display a strong mutual relation with respect to this observable. This so-called quantum entanglement means that although the outcomes of the observables measured cannot be predicted with certainty for each of the two EPR systems, the outcomes of the observables for any arbitrary measurement of the complete system is always strictly correlated. From this, it can be generalised that quantum entanglement violates the concept of a unique physical reality of nature [1]. This differs from the classical notion of reality since the individual result of the correlated system is essentially undetermined before the measurement is undertaken. Furthermore, according to quantum mechanics, the measurement of a certain observable in one EPR system instantaneously

determines the state of the other observable, regardless of the distance between the systems.

The conflict between local realism and quantum mechanics resulted in the development of a quantitative test to understand this phenomenon known as the Bell's inequalities [2]. This test states that by any local and realistic theory, there exist a set of inequalities which must be satisfied. Quantum mechanics, however, predicts the violation of these Bell's inequalities for measurements on specific quantum-entangled systems. An experimental realization of the Bell's inequalities, presented by Clauser, Horne, Shimony and Holt (CHSH), showed a classical argument that bounds the correlation of two particles. Entanglement can be verified as applied to quantum-entangled photons, for example, by violating this argument [3].

One method of generating entangled pairs occurs through a process known as Spontaneous Parametric Down Conversion (SPDC), first established by David Burham and Donald Weinberg. They showed that by pumping a non-linear crystal they were able to split a photon into two single photons known as a signal and an idler [4]. During this process, the conservation of momentum and energy are obeyed such that the additive energy of the signal and idler is equal to

*205513117@stu.ukzn.ac.za

the energy of the pump photon and similarly for the momentum.

Some other methods of obtaining entanglement do exist, such as the use of quantum dots [5], exploiting atomic cascades [6] and recently through the use of four-wave mixing in chip-scale micro-resonators [7-9]. Entanglement is at the core of quantum information science [10-11], which branches out into many applications explicitly quantum computing [12-15], quantum teleportation [16-17] and quantum cryptography [18]. Of interest is the use of entanglement for the development of quantum repeaters, which is applicable to the advancement of quantum communication by enhancing the quantum key distribution process [19-21].

This paper is structured to begin with a brief overview of the theory of entanglement (Sec. 2). A description of the assembly of a polarization-based entanglement source is provided in Sec. 3 and the results and analysis that proved entanglement are presented in Sec. 4. A summary of conclusion is presented in Sec. 5.

2. Theory

When considering the behavior of a quantum system such as a photon, it is represented by a probabilistic wave function whereby the properties of the photon are unknown, however, it can be represented as a probabilistic distribution denoted as

$$|\psi\rangle = \alpha|0\rangle + \beta|1\rangle \tag{1}$$

Where, α and β are the complex coefficients well-defined by the normalization condition $|\alpha|^2 + |\beta|^2 = 1$. The properties of the photon are defined in terms of the correlated observables as described by the Heisenberg's uncertainty principle. These properties remain indefinite until an observation, which collapses the wave function, has been made. Photons, which are entangled, are considered indistinguishable and are therefore represented as a single state. This means that for a complete description of any component within an entangled system, the description of its entangled partner is also included. This also implies that there exists a strong mutual correlation between maximally entangled photon pairs, as mentioned previously.

For the purpose of this study, we will concentrate on a polarisation based entanglement source since it is independent of the change of

orientation during propagation within a free-space system under turbulent conditions [22]. A photon pair which is entangled via polarization can be represented either by the rectilinear (horizontal and vertical) or the diagonal (+/- 45 degrees) bases denoted as:

$$|\psi\rangle = \frac{1}{\sqrt{2}} [|V\rangle_s |V\rangle_i + e^{i\phi} |H\rangle_s |H\rangle_i] \tag{2}$$

Where, $|V\rangle$ and $|H\rangle$ are the vertical and horizontal states respectively and s and i denote the signal and idler [23]. Coincidence is evaluated via the single count rates at each detector and is defined as:

$$C = \frac{(N_a)(N_b)(t_c)}{\tau} \tag{3}$$

Where, C is the coincidence determined from N_a and N_b , which are the single counts measured at detectors A and B, respectively, t_c is the time resolution, which is an indication of how far apart incidents must be for the system to register them, and τ is the gated time [23]. The practicality of coincidence counts shall be discussed further in sections 3 and 4 when quantifying the degree of entanglement within an optical system.

2.1. Testing for entanglement

Prior to verifying entanglement by observing the violation of the CHSH inequality, a test of visibility is used to determine the correlation of the entangled photon pairs. This is measured in both bases by considering the maximum and minimum coincidence according to condition

$$V = \frac{C_{\max} - C_{\min}}{C_{\max} + C_{\min}} \tag{4}$$

Where, V corresponds to the visibility for a given basis and C_{\max} and C_{\min} are the maximum and minimum coincidence rates, respectively. The error ΔV on the visibility is determined by applying the Gaussian error propagation rule

$$\Delta V = \sqrt{\left(\frac{\partial V}{\partial C_{\max}} \Delta C_{\max}\right)^2 + \left(\frac{\partial V}{\partial C_{\min}} \Delta C_{\min}\right)^2} \tag{5}$$

Where

$$\frac{\partial V}{\partial C_{\max}} = \frac{2C_{\min}}{(C_{\max} + C_{\min})^2}$$

and

$$\frac{\partial V}{\partial C_{\min}} = \frac{2C_{\max}}{(C_{\max} + C_{\min})^2}$$

The acquired coincidence rates are assumed to be statistically independent Poisson random variables, so that $\Delta C_{\max} = \sqrt{C_{\max}}$ and $\Delta C_{\min} = \sqrt{C_{\min}}$.

The verification of entanglement however lies in the violation of the CHSH inequality, which states that in local realistic theories the absolute value of a particular combination of correlations

$$E[\alpha, \beta] = \frac{C(\alpha, \beta) - C(\alpha_{\perp}, \beta) - C(\alpha, \beta_{\perp}) + C(\alpha_{\perp}, \beta_{\perp})}{C(\alpha, \beta) + C(\alpha_{\perp}, \beta) + C(\alpha, \beta_{\perp}) + C(\alpha_{\perp}, \beta_{\perp})} \tag{7}$$

Where, $C(\alpha, \beta)$ denotes the coincidence count rate obtained for the combination of polarizer settings and α_{\perp} and β_{\perp} are the perpendicular polarization orientation. The statistical nature of the inequality requires that sufficiently long integration time for collecting the required coincidence rates. The standard deviation of the experimental value is obtained by applying the sum rule represented as follows

$$\Delta E(a, b) = 2 \left[\frac{[C(\alpha, \beta) + C(\alpha_{\perp}, \beta_{\perp})][C(\alpha, \beta_{\perp}) + C(\alpha_{\perp}, \beta)]}{C(\alpha, \beta) + C(\alpha_{\perp}, \beta) + C(\alpha, \beta_{\perp}) + C(\alpha_{\perp}, \beta_{\perp})} \right] \times \left[\frac{1}{\sqrt{C(\alpha, \beta) + C(\alpha_{\perp}, \beta_{\perp})}} + \frac{1}{\sqrt{C(\alpha_{\perp}, \beta) + C(\alpha, \beta_{\perp})}} \right] \tag{9}$$

2.2. Accounting for the fidelity of the generated states

A pure SPDC entangled state should ideally be generated however this is highly unlikely due to experimental errors. For this reason, the purity of the generated states is determined by performing a state tomography. By constructing the two-photon density matrix and considering the interference effect of two photons, the fidelity of the system is determined. This is achieved experimentally by assembling an interferometer to verify the interference of two indistinguishable photons at a non-polarizing beam-splitter. This phenomenon is known as the Hong-Ou-Mandel interference [24].

between two particles is bounded by 2, such that the violation is represented as

$$S(\alpha, \alpha', \beta, \beta') = E[\alpha, \beta] - E[\alpha, \beta'] + E[\alpha', \beta] + E[\alpha', \beta'] \leq 2 \tag{6}$$

Where, α and α' , and β and β' denote the local measurement settings of the two observers, respectively, each receiving one of the entangled particles. The normalized expectation value $E[\alpha, \beta]$ is given by

$$S(\alpha, \alpha', \beta, \beta') = \sqrt{\sum_{a=\alpha, \alpha'} \sum_{b=\beta, \beta'} \Delta E(a, b)^2} \tag{8}$$

Where, the errors $\Delta E(a, b)$ on the individual correlation coefficients are computed via Gaussian error propagation as

In the case where two photons impinge on a 50:50 beam-splitter, four outcomes are possible as represented in Fig. 1. Either both the photons (A and B) are transmitted (1a), both photons are reflected (1b), photon A is transmitted while the photon B is reflected (1c), and vice versa (1d).

When both detectors at the output of the beam-splitter register photons in coincidence, as in Figs. 1a and 1b, the photons are indistinguishable since they have the same wavelength, polarization and spatial-temporal mode. In the case of Figs. 1c and 1d, however, where only a single detector will see photons, no coincidence counts would result.

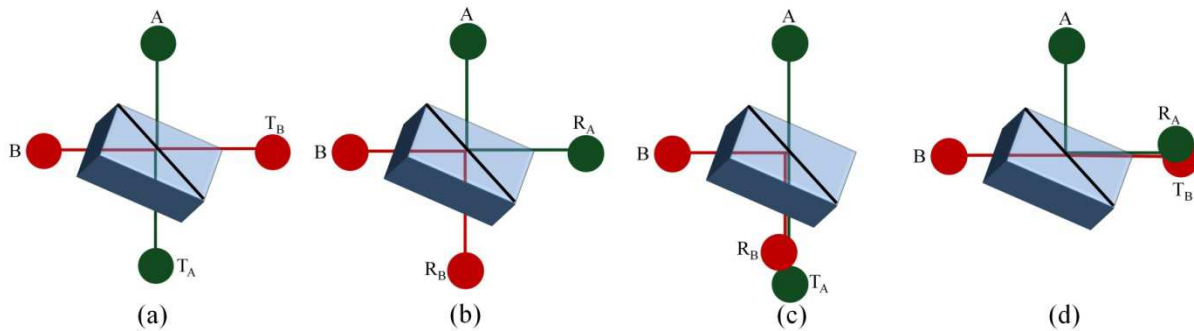


Fig.1: Four possible paths travelled by two photons impinging on a balanced non-polarizing beam-splitter. Both photons (A and B) are either transmitted (a) or reflected (b). Alternatively photon A is transmitted while photon B is reflected (c) or vice versa (d).

Using the aforementioned interferometer a state tomography can be used to reconstruct the density matrix of an unknown quantum state. In the case of entangled photon pairs the state tomography requires a set of 16 projective measurements. These are specified by all possible combination of projecting the two photons into either $|H\rangle$, $|V\rangle$ plus diagonal $|P\rangle$ or right circular $|R\rangle$ states where $|P\rangle$ and $|R\rangle$ are defined, respectively, as

$$|P\rangle = \frac{1}{\sqrt{2}} [|H\rangle + |V\rangle] \tag{10}$$

and

$$|R\rangle = \frac{1}{\sqrt{2}} [|H\rangle + i|V\rangle] \tag{11}$$

These are possible pure polarization states constructed from the superposition of $|H\rangle$ and $|V\rangle$. To quantitatively characterize the fidelity of the system, the deviation of the experimental density matrix from the ideal case is considered. This is determined by taking into account the overlap of the experimental density matrix with respect to the theoretical density matrix [25] and represented as

$$F = Tr \left[\left(\sqrt{\rho_{th}} \rho_{exp} \sqrt{\rho_{th}} \right)^{\frac{1}{2}} \right] \tag{12}$$

Where, F is the fidelity, which takes a value between 0 and 1, ρ_{exp} is the experimentally obtained density matrix and ρ_{th} is the theoretically calculated density matrix, which is defined to be the Bell state. The maximum value of 1 is obtained

if $\rho_{exp} = \rho_{th}$, which implies that the two states are completely indistinguishable. The mapping of the tomographic density matrix is given by

$$\rho = \frac{\sum_{v=1}^{16} M_v C_v}{\sum_{v=1}^4 C_v} \tag{13}$$

Where, c_v is the coincidence counts for each of the 16 projections and M_v is defined below, where $B_{v,\mu} = \langle \Psi_v | \Gamma_\mu | \Psi_v \rangle$ [25]

$$M_v = \sum_{\mu=1}^4 (B^{-1})_{v,\mu} \Gamma_\mu \tag{14}$$

3. Methodology of Generation and Verification of Entanglement

To demonstrate entanglement, a simple optical system can be constructed whereby the most important component is the non-linear crystal, which is responsible for the down conversion of photons into single photon pairs. A schematic of the polarization based entangled source can be found in Fig. 2. Within this scheme, a UV laser ($\lambda=404$ nm) with an output power of 20 mW was used to pump two type I beta-Barium Borate (BBO) crystals. For the purpose of alignment, the beam was propagated through spherical and cylindrical lenses, respectively, onto a Half Wave Plate (HWP), which compensated for the phase shift caused by the two spatially separated BBO crystals.

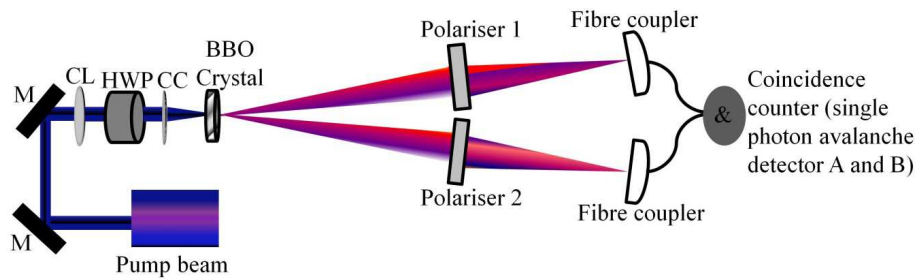


Fig.2: Schematic of an entangled photon source comprising of a pump laser lasing as 404 nm, alignment optics (mirror (M) and cylindrical lens (CL)), a Half Wave Plate (HWP), a Crystal Compensator (CC), BBO crystal, a polarizer in each arm followed by a fiber coupler connected to a coincidence counter comprising of single photon avalanche detectors A and B via polarization maintaining fibers.

The photons of the pump beam ($\lambda = 404 \text{ nm}$) upon encountering the BBO crystal have a small possibility ($\approx 10^{-11}$ for standard material) of being absorbed into a higher energy level and thereafter re-emitted into a pair of single photons to a lower energy level (ground state) at a wavelength of 808

nm. The single photon pair generated is thus referred to as a signal and the idler. As mentioned previously, during this process, energy and momentum is conserved since the crystal remained in an unaltered state as illustrated in Fig. 3.

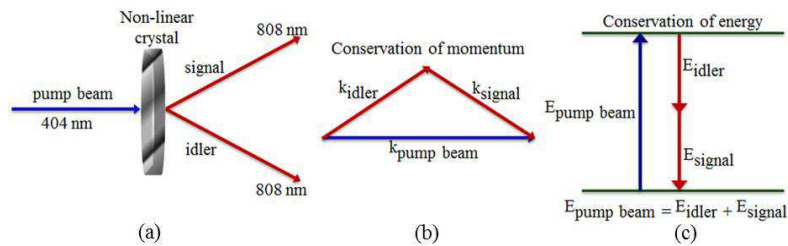


Fig.3: During the process of SPDC pump photons are down converted into a signal and an idler with a longer wavelength. During this process the BBO crystal remains unaltered hence momentum (b) and energy (c) are conserved.

Within the aforementioned optical scheme, the two BBO crystals were mounted orthogonal with respect to each other. The first BBO crystal was responsible for the generation of vertically polarized photon pairs while the second one accounted for the generation of the horizontally polarized photon pairs. This simply means there was an equal probability that a pump photon will be down converted in either of the crystals when the crystal was pumped with linearly polarized light at 45° , resulting in the generation of the desired state, which was required to test for the violation of the CHSH inequality as represented by Eqn. (2) and further illustrated in Fig. 4.

Since the entangled properties of the photon pair, namely its state of polarization, remains unknown until a measurement is carried out, we

placed polarizers in each arm to determine the state of polarization of the photon pairs. The single photons were detected via a coupler connected through polarization maintaining fibers to a coincidence counter embedded with avalanche photon detectors. This system, as described, can be used to verify the visibility of both rectilinear and diagonal bases and test for entanglement by violating the CHSH inequality. However, to test the fidelity of the system, some adaptation of the system is required. This was observed by considering the interference of the photon pairs generated. For the purpose of the experimental demonstration of the distinguishability of the photons pairs, instead of constructing a traditional interferometer, a balanced beam-splitter is assembled by making use of a fused 50:50

polarization maintaining fiber coupler. The adaptation of the optical system is represented in Fig. 5 whereby the photon pairs were directed towards a 50:50 polarization maintaining fiber coupler, which was used as a beam-splitter, via a transmitting collimator. Either arms of the two photon interferometer contained a short free-space optical line. The length of one of the optical lines remained fixed while the other line was varied by means of a manual micrometer translation stage. This made it possible to tune the path difference between the two optical arms in order to record the

interference dip. The output of the 50:50 polarization maintaining fiber coupler were connected via a receiving collimator to the coincidence counter by means of a polarization maintaining fiber in order to measure the coincidence. A HWP and QWP are placed in both arms to vary the polarization. This will assist in obtaining the coincidence counts for the various projective permutation required to reconstruct the density matrix from which the fidelity of the system was determined.

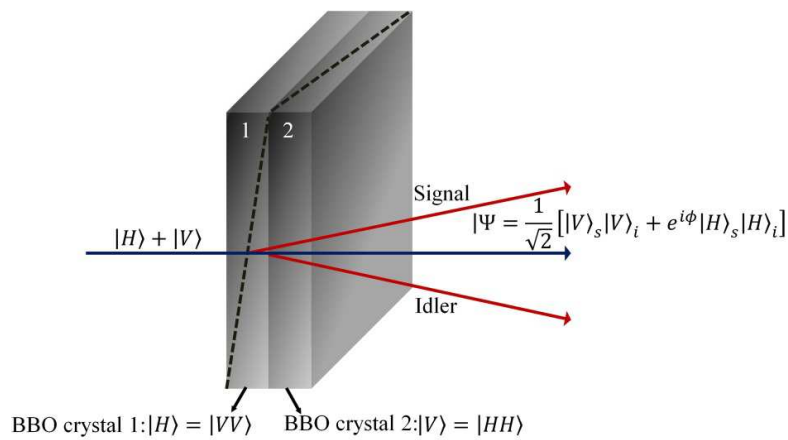


Fig.4: State preparation through two type I non-linear crystals.

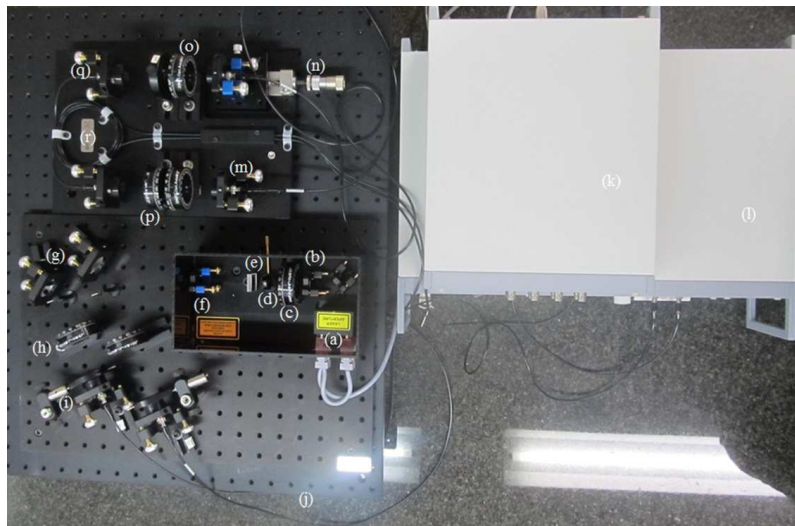


Fig.5: Optical system constructed to generate and characterize single photon pairs: (a) UV pump laser lasing at 404 nm, (b) spherical lens, (c) Half Wave Plate (HWP), (d) receiving collimators, (e) Quarter Wave Plate (QWP), (f) HWP, (g) receiving collimator and (r) is the 50: 50 polarization maintaining fiber coupler. (h) is the 50: 50 polarization maintaining fiber coupler, (i) manual micrometer translation stage, (j) transmitting collimators, (k) Time to digital convertor, (l) coincidence counter embedded with single photon detectors, (m) transmitting collimators, (n) manual micrometer translation stage (o) Quarter Wave Plate (QWP), (p) HWP, (q) receiving collimator and (r) is the 50: 50 polarization maintaining fiber coupler.

4. Results and Discussion

A test for entanglement of photon pairs involves a measurement of correlation curves in two non-orthogonal bases, the rectilinear and the diagonal bases. This was observed by setting the orientation of polarizer 1 in Fig. 2 to 0 degrees for the rectilinear basis and 45 degrees for the diagonal

basis and thereafter varying the orientation of polarizer 2 while measuring the coincidence at each orientation. This verified the correlation relationship that exists between the two bases as illustrated in Fig. 6.

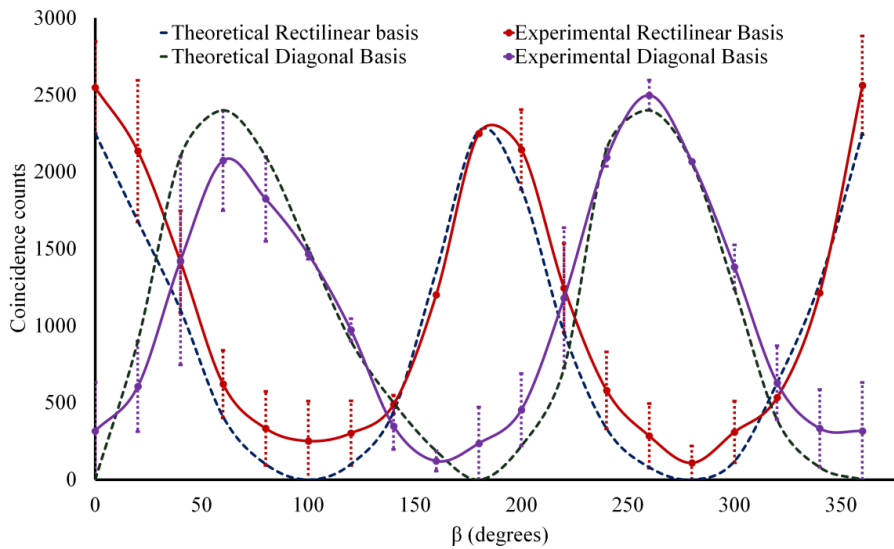


Fig.6: Plot representing the correlation of the rectilinear and diagonal bases. The dashed line is the theoretical prediction whilst the solid lines represent the experimental data obtained.

As observed, we verified that the coincidence counts of both bases (rectilinear and diagonal) have cosine squared dependence and they are correlated. The resultant visibility was measured to be $91.0 \pm 0.8 \%$ and $91.0 \pm 0.8 \%$ for the rectilinear and diagonal basis, respectively, which was deduced from Eqn. (4).

To test for the violation, the following set of orientation were chosen, $\alpha = 0^\circ$, $\alpha' = 45^\circ$, $\beta = 22.5^\circ$ and $\beta' = 67.5^\circ$. Four separate experimental runs were conducted corresponding to four terms $E[\alpha, \beta]$ in the definition of S . Each of the $E[\alpha, \beta]$ term is calculated from four numbers of coincidences, making it collectively 16 count rates. Using the data obtained during the various experimental runs, as illustrated in Table 1, the violation was measured to be 2.71 ± 0.03 , which verified entanglement. The theoretical limit for the

violation of the CHSH inequality is $2\sqrt{2}$ and we obtained a value within 3.56 % deviation of the expected value. This could be due to slight misalignment of our systems. At lower integration time, the coincidence counts tend to fluctuate, which will result in accidental counts. This will also lower the S-value obtained.

Although this verified entanglement, as a last step in the characterization of a polarization-based entangled source, the fidelity of the system was tested. This was achieved by setting the HWP and QWP to the appropriate orientation as listed in Table 2 and measuring the coincidence at each permutation. Using Eqn. (13) the density matrix of the system was reconstructed to be

$$\rho_{\text{exp}} = \begin{bmatrix} 0.4407 & 0.0035 - 0.0416i & 0.0788 + 0.0876i & 0.5511 + 0.0450i \\ 0.0035 + 0.0416i & 0.0060 & -0.0515 + 0.0745i & -0.0850 - 0.0382i \\ 0.0788 - 0.0876i & -0.0515 - 0.0745i & 0.0082 & 0.1429 + 0.0856i \\ 0.5511 - 0.0450i & -0.0850 + 0.0322i & 0.1429 - 0.0856i & 0.5450 \end{bmatrix}$$

Table 1: Data collected for the experimental runs to verify entanglement.

Expectation value when α is 0 and β is 22.5 degrees								
α	β	α_{\perp}	β_{\perp}	$C(\alpha, \beta)$	$C(\alpha_{\perp}, \beta)$	$C(\alpha, \beta_{\perp})$	$C(\alpha_{\perp}, \beta_{\perp})$	$E(\alpha, \beta)$
0	22.5	90	112.5	8557	1838	1886	8939	0.649
Expectation value when α' is 45 and β is 22.5 degrees								
α'	β	α'_{\perp}	β_{\perp}	$C(\alpha', \beta)$	$C(\alpha'_{\perp}, \beta)$	$C(\alpha', \beta_{\perp})$	$C(\alpha'_{\perp}, \beta_{\perp})$	$E(\alpha', \beta)$
45	22.5	135	112.5	11296	2253	1041	10442	0.737
Expectation value when α is 0 and β' is 67.5 degrees								
α	β'	α_{\perp}	β'_{\perp}	$C(\alpha, \beta')$	$C(\alpha_{\perp}, \beta')$	$C(\alpha, \beta'_{\perp})$	$C(\alpha_{\perp}, \beta'_{\perp})$	$E(\alpha, \beta')$
0	67.5	90	15.5	2950	10707	7238	1642	-0.592
Expectation value when α' is 45 and β' is 67.5 degrees								
α'	β'	α'_{\perp}	β'_{\perp}	$C(\alpha', \beta')$	$C(\alpha'_{\perp}, \beta')$	$C(\alpha', \beta'_{\perp})$	$C(\alpha'_{\perp}, \beta'_{\perp})$	$E(\alpha', \beta')$
45	67.5	135	157.5	13180	1697	2070	11211	0.732

Table 2: Experimental data for the various polarization projections used to determine the fidelity of the system.

v	State 1	State 2	HWP 1	QWP 1	HWP 2	QWP 2	C
1	$ H\rangle$	$ H\rangle$	45	0	45	0	23 464
2	$ H\rangle$	$ V\rangle$	45	0	0	0	320
3	$ V\rangle$	$ V\rangle$	0	0	0	0	29 018
4	$ V\rangle$	$ H\rangle$	0	0	45	0	439
5	$ R\rangle$	$ H\rangle$	22.5	0	45	0	16 618
6	$ R\rangle$	$ V\rangle$	22.5	0	0	0	12 636
7	$ P\rangle$	$ V\rangle$	22.5	45	0	0	10 141
8	$ P\rangle$	$ H\rangle$	22.5	45	45	0	16 145
9	$ P\rangle$	$ R\rangle$	22.5	45	22.5	0	16 216
10	$ P\rangle$	$ P\rangle$	22.5	45	22.5	45	35 426
11	$ R\rangle$	$ P\rangle$	22.5	0	22.5	45	14 225
12	$ H\rangle$	$ P\rangle$	45	0	22.5	45	12 079
13	$ V\rangle$	$ P\rangle$	0	0	22.5	45	10 256
14	$ V\rangle$	$ L\rangle$	0	0	22.5	90	10 170
15	$ H\rangle$	$ L\rangle$	45	0	22.5	90	14 109
16	$ R\rangle$	$ L\rangle$	22.5	0	22.5	90	24 412

A graphical representation of the real part of the density matrix is illustrated in Fig. 7. The fidelity of the system was determined to be 0.997 ± 0.0001 , which was evaluated using Eqn. (12) and taking the trace of the density matrix. Noticeably the fidelity is almost 1, which means that the states are indistinguishable and that the quantum states are well preserved.

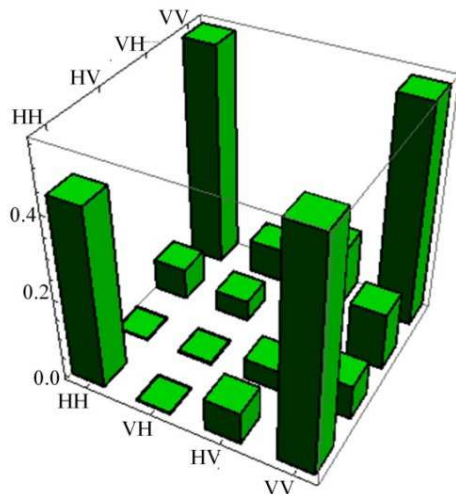


Fig.7: Graphical representation of the real part of the reconstructed density matrix.

5. Conclusion

We have thus shown that it was possible to generate polarization based entangled photon pairs and characterize them by measuring the visibility of the correlation curves of rectilinear and diagonal bases. We also proved that our system was entangled since we were able to violate the CHSH inequality. Carrying out the state tomography revealed that the quantum state remained preserved during propagation. We have thus illustrated a simple process of generating and characterizing entangled single photon pairs. Entanglement is beneficial for the development of quantum communication based technologies, which include quantum key distribution and quantum computing. If successfully implemented, these processes would lead to a shift in the approach that the security of information is dealt with to date.

Acknowledgements

This work is based on research supported by the South African Research Chair Initiative of the Department of Science and Technology, National

Research Foundation and Council for Scientific and Industrial Research.

References

- [1] A. Einstein, B. Podolsky and N. Rosen, *Phys. Rev.* **47**(10), 777 (1935).
- [2] J. S. Bell, *Physics* (Long Island City, N.Y.) **1**, 195 (1964).
- [3] J. Clauser, R. Holt, M. Horne and A. Shimony, *Physics Review Letters* **23**(15), 880 (1969).
- [4] D. C. Burnham and D. L. Weinberg, *Physics Review Letters* **25**, 84 (1970).
- [5] A. Muller, W. Fang, J. Lawall and G. S. Solomo, *Physics Review Letters* **103**, 217 (2009).
- [6] C. A. Kocher and E. D. Commins, *Physics Review Letters* **18**(15), 575 (1967).
- [7] S. Clemmen, K. P. Huy, W. Bogaerts, R. G. Baets, P. Emplit and S. Massar, *Optics Express* **17**, 16558 (2009).
- [8] L. G. Helt, Z. Yang, M. Liscidini and J. E. Sipe, *Optics Letters* **35**, 3006 (2010).
- [9] J. Chen, Z. H. Levine, J. Fan and A. L. Migdall, *Optics Express* **19**, 1470 (2011).
- [10] I. Chuang and M. Nielsen, *Quantum Computation and Quantum Information*, tenth edition (Cambridge, University Press, 2000).
- [11] D. Bouwmeester, A. Ekert and A. Zeilinger, *The Physics of Quantum Information*, first edition (Springer-Verlag, Berlin, Heidelberg, 2000).
- [12] C. F. Roos et al., *Science* **304**, 1478 (2004).
- [13] J. Chiaverini et al., *Science* **308**, 997 (2005).
- [14] D. Schrader et al., *Physics Review Letters* **93**, 150501 (2004).
- [15] R. Raussendorf and H. J. Briegel, *Physics Review Letters* **86**, 5188 (2001).
- [16] C. H. Bennett et al., *Physics Review Letters* **70**, 1895 (1993).
- [17] D. Bouwmeester et al., *Nature* **390**, 575 (1997).
- [18] A. Ekert, *Phys. Rev. Lett.* **67**, 661 (1991).
- [19] H. J. Briegel et al., *Physics Review Letters* **81**, 5932 (1998).
- [20] S. Bratzik et al., *Physics Review A* **87**, 062335 (2013).
- [21] N. Curtz et al., *Optics Express* **18**(21), 22099 (2010).
- [22] R. L. Fante, *Proc. of IEEE* **63**(12), 1669 (1975).
- [23] D. Dehlinger and M. W. Mitchell, *American J. Physics* **70**(9), 903 (2002).

- [24] C. K. Hong, Z. Y. Ou and L. Mandel, Physics Review Letters **59(18)**, 2044 (1987).
- [25] D. F. V. James et al., Physics Review A **64**, 052312 (2001).

Received: 12 March, 2014

Accepted: 18 July, 2014